Investigation of the Beta-Spectra of Be^{10}, K^{40}, Tc^{99}, and Cl^{36}†

L. FELDMAN AND C. S. WU
Columbia University, New York, New York

(Received May 22, 1952)

The beta spectra of Be^{10}, K^{40}, Tc^{99}, and Cl^{36} were investigated with the Columbia University solenoidal spectrometer and it was found that each exhibited a forbidden shape. An analysis of the spectra yields the following results. The spectrum of Be^{10}, for which $\Delta J=3$, can be explained equally well by $2T$ or $2A$ for no parity change and by $3T$ or $3V$ if the parity does change. Similarly, the spectrum of K^{40}, for which $\Delta J=4$, can be accounted for by $3T$ or $3A$ if the parity changes and by $4T$ or $4V$ for no parity change. $\Delta J=2$ for the decays of both Tc^{99} and Cl^{36}. These spectra can be explained only by $2T$ or $2V$ with values for k^2 of 45 for Tc^{99} and 18 for Cl^{36} ($k^2=|A_{ij}|^2\div|T_{ij}|^2$). If the true interaction prevailing in beta-decay is but a single one of the five linearly independent interactions, then it follows from these spectrum analyses that it must be the tensor interaction. A linear combination of tensor with one or more of the other interactions is possible. It seems, however, that more information than is provided by spectrum studies alone is necessary to determine the exact form of such a linear combination.

I. INTRODUCTION

THIS paper reports the results on the main portion of the investigation of forbidden beta-spectra begun in 1948 with the Columbia University solenoidal spectrometer. Preliminary results on the spectra of Be^{10},[1] K^{40},[2] Tc^{99},[3] and Cl^{36} [4] have been reported at several meetings of the American Physical Society and in various publications.[5] The measurements of the Cl^{36} spectrum presented in this paper were made with sources greatly improved in uniformity and thinness over those used in our earlier work,[4] thus extending the reliability of the data to much lower energies than was previously possible.

The momentum distribution of the electrons emitted in beta-decay is given by the Fermi theory as

$$P(p)dp=(G^2/2\pi^3)C_{nX}F(Z,W)p^2q^2dp, \qquad (1)$$

with $p^2=W^2-1$ and $q=W_0-W$. We will use the notation of Konopinski and Uhlenbeck[6] with the generalized expression for C_{nX} given by Greuling.[7] C_{nX} is the factor by which the allowed distribution must be multiplied to give a forbidden spectrum. It contains the matrix elements of the interaction between the nucleons and the beta-neutrino field in which appear factors dependent on the beta-energy, W and Z. n refers to the degree of forbiddenness and X to the interaction form. The essence of the Fermi theory is that the interaction giving rise to beta-decay is assumed to be proportional to the scalar product of relativistically invariant bilinear combinations of the wave functions of the neutrino and beta-particle and of the initial and final nuclei involved in the beta-process.[8] Fermi originally chose the form which transforms as a polar vector, but there are five possible linearly independent bilinear combinations which are relativistically invariant. These are classified according to their transformation properties and will be denoted by their usual abbreviations S, V, T, A, and P. The correct interaction may be none of these, but if it is to be Lorentz invariant and linear in the four wave functions involved, then it must be expressible as a linear combination of the five linearly independent forms. The properties of such a linear combination, except for interference effects, can be analyzed in terms of the properties of the individual forms.

For the allowed spectra, all the C_{0X} are constant, and therefore the energy dependence is completely given by the Coulomb factor, $F(Z, W)$, and the statistical factor p^2q^2dp describing the distribution of the decay energy between the beta-particle and the neutrino. Thus any theory which includes the neutrino concept and yields energy independent nuclear matrix elements to the first order could account for the experimentally observed shapes of the allowed spectra as well as the Fermi theory. Therefore, the investigation of the forbidden spectra will provide a decisive test of the theory and further select or limit the choice of the particular interaction form prevailing in beta-decay from the five linearly independent Lorentz invariant forms or linear combinations thereof.

The following is a condensation of the expressions given by Greuling[7] for C_{nX} and the appropriate selection rules:

† This work was made possible through partial support of the USAEC.

[1] C. S. Wu and L. Feldman, Phys. Rev. **76**, 698 (1949); L. Feldman and C. S. Wu, Phys. Rev. **78**, 318 (1950).
[2] L. Feldman and C. S. Wu, Phys. Rev. **81**, 298 (1951).
[3] C. S. Wu and L. Feldman, Phys. Rev. **82**, 332 (1951).
[4] C. S. Wu and L. Feldman, Phys. Rev. **76**, 693 (1949); **82**, 457 (1951).
[5] C. S. Wu, Revs. Modern Phys. **22**, 386 (1950); Proc. Intern. Conf. of Nuc. Phys., University of Chicago, 1951.
[6] E. J. Konopinski and G. E. Uhlenbeck, Phys. Rev. **60**, 308 (1941).
[7] E. Greuling, Phys. Rev. **61**, 568 (1942).
[8] A complete review of the theory of beta-decay is given by E. J. Konopinski, Revs. Modern Phys. **15**, 209 (1943).

$$
\begin{aligned}
C_{nS}&=S_{n,(n-1)'}(\beta\mathbf{r},\mathbf{r})\,|\,Q_n(\beta\mathbf{r},\mathbf{r})/n!\,|^2,\\
C_{nP}&=P_{n,(n-1)'}(\beta\gamma_5\mathbf{r},\mathbf{r})\,|\,Q_n(\beta\gamma_5\mathbf{r},\mathbf{r})/n!\,|^2,\\
C_{nV}&=V_{n,(n-1)'}(\mathbf{r},\mathbf{r})\,|\,Q_n(\mathbf{r},\mathbf{r})/n!\,|^2\\
&\quad+V_{n,(n-1)'}(\boldsymbol{\alpha},\mathbf{r})\,|\,Q_n(\boldsymbol{\alpha},\mathbf{r})/n!\,|^2\\
&\quad+iV_{n,(n-1)'}(\mathbf{r},\mathbf{r}:\boldsymbol{\alpha},\mathbf{r})[Q_n(\boldsymbol{\alpha},\mathbf{r})\cdot Q_n^*(\mathbf{r},\mathbf{r})\\
&\quad-\text{c.c.}]/(n!)^2+V_{n-1}([\boldsymbol{\alpha}\times\mathbf{r}],\mathbf{r})\\
&\qquad\times|\,Q_{n-1}([\boldsymbol{\alpha}\times\mathbf{r}],\mathbf{r})/(n-1)!\,|^2,\\
C_{nT}&=T_n(\beta[\boldsymbol{\sigma}\times\mathbf{r}],\mathbf{r})\,|\,Q_n(\beta[\boldsymbol{\sigma}\times\mathbf{r}],\mathbf{r}/n!\,|^2\\
&\quad+T_n(\beta\boldsymbol{\alpha},\mathbf{r})\,|\,Q_n(\beta\boldsymbol{\alpha},\mathbf{r})/n!\,|^2\\
&\quad-T_n(\beta\boldsymbol{\alpha},\mathbf{r}:\beta[\boldsymbol{\sigma}\times\mathbf{r}],\mathbf{r})[Q_n(\beta[\boldsymbol{\sigma}\times\mathbf{r}],\mathbf{r})\\
&\quad\cdot Q_n^*(\beta\boldsymbol{\alpha},\mathbf{r})+\text{c.c.}]/(n!)^2+T_{n',(n+1)}(\beta\boldsymbol{\sigma},\mathbf{r})\\
&\qquad\times|\,Q_{n+1}(\beta\boldsymbol{\sigma},\mathbf{r})/(n+1)!\,|^2,\\
C_{nA}&=A_n([\boldsymbol{\sigma}\times\mathbf{r}],\mathbf{r})\,|\,Q_n([\boldsymbol{\sigma}\times\mathbf{r}],\mathbf{r})/n!\,|^2\\
&\quad+A_{n',(n+1)}(\boldsymbol{\sigma},\mathbf{r})\,|\,Q_{n+1}(\boldsymbol{\sigma},\mathbf{r})/(n+1)!\,|^2.
\end{aligned}
\tag{2}
$$

The energy dependent factors as given by Greuling are represented here by the capital letters, $S_{n,(n-1)'}(\beta\mathbf{r},\mathbf{r})$, etc., denoting the particular interaction in which they occur. The expressions in parentheses identify the matrix elements, the Q_n's, with which each correction factor is associated. The subscripts n, $n-1$, and $n+1$ indicate the selection rules which apply for each matrix element. Thus the particular matrix element is non-vanishing in the nth forbidden approximation unless ΔJ is equal to one of the values in the subscript. A prime subscript signifies that the additional requirement $|J_i|+|J_f|>\Delta J$ must be satisfied. Thus, for example, a matrix element with the selection rule $\Delta J=n'$ does not appear in $n\rightarrow 0$ transitions. The selection rule for the change in parity is no for n even and yes for odd n in all cases except for C_{nP} in which the reverse is true. The expressions for C_{nX} as given by Greuling and above are complete except for certain matrix elements which appear in C_{1T}, C_{2T}, and C_{1A}, for which the selection rule is $\Delta J=0$, and do not apply to any of the forbidden spectra discussed in this paper. Also omitted are terms of $n+2$ order of magnitude which constitute negligible corrections to the nth forbidden approximation.

Certain general remarks can be made about the energy dependent factors. $S_n(\beta\mathbf{r},\mathbf{r})$ and $P_n(\beta\gamma_5\mathbf{r},\mathbf{r})$ are identical and also practically impossible to distinguish

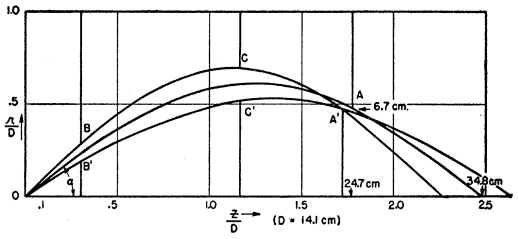

FIG. 1. Ring-focus baffle for solenoid spectrometer, showing various baffle positions and typical particle trajectories plotted in $r-Z$ plane.

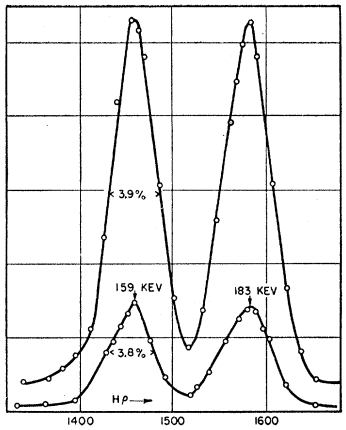

FIG. 2. Internal conversion line of In^{114} taken with ring-focus baffle and with Witcher-Haggstrom baffle. Ratio of peaks is 3.7.

experimentally from $V_n(\mathbf{r},\mathbf{r})$, $T_n(\beta[\boldsymbol{\sigma}\times\mathbf{r}],\mathbf{r})$, and $A_n([\boldsymbol{\sigma}\times\mathbf{r}],\mathbf{r})$. $V(\boldsymbol{\alpha},\mathbf{r})$ and $T(\beta\boldsymbol{\alpha},\mathbf{r})$ are identical for given n, as are $T(\beta\boldsymbol{\sigma},\mathbf{r})$ and $A(\boldsymbol{\sigma},\mathbf{r})$. $V(\boldsymbol{\alpha},\mathbf{r})$ and $T(\beta\boldsymbol{\alpha},\mathbf{r})$ for given degree of forbiddenness, n, are the same as $T(\beta\boldsymbol{\sigma},\mathbf{r})$ and $A(\boldsymbol{\sigma},\mathbf{r})$ for n one degree lower, i.e., if $n=m+1$, then

$$V_n(\boldsymbol{\alpha},\mathbf{r})=T_n(\beta\boldsymbol{\alpha},\mathbf{r})=T_{m+1}(\beta\boldsymbol{\sigma},\mathbf{r})=A_{m+1}(\boldsymbol{\sigma},\mathbf{r}).$$

Generally there is considerable arbitrariness in applying the C_{nX} to a particular spectrum because the magnitudes of the nuclear matrix elements are not known. The practice is to adjust the ratios of the matrix elements to give the best fit to the experimental data. This arbitrariness does not exist if $\Delta J=n+1$ in which case all the matrix elements vanish except the ones with the factors $T(\beta\boldsymbol{\sigma},\mathbf{r})$ and $A(\boldsymbol{\sigma},\mathbf{r})$. Thus only the T or A interactions can account for such a decay and the spectral shape predicted by the theory is unique since only one matrix element is involved with the well-defined energy factor, $A_{n+1}(\boldsymbol{\sigma},\mathbf{r})=T_{n+1}(\beta\boldsymbol{\sigma},\mathbf{r})$. A convenient method illustrating the selection rules is to regard the change in the total angular momenta of the parent and product nuclei, ΔJ, to be equal to the sum of the orbital plus spin angular momenta carried away by the neutrino and beta-particle. Thus $\Delta J=\Delta L+\Delta S$. ΔL determines the degree of forbiddenness and the change in parity, since $n=\Delta L$. The beta- and neutrino each have a spin of $\frac{1}{2}$, and thus $\Delta S=0$ or 1. For the case $\Delta J=n+1$, $\Delta S=1$ and only those matrix elements which contain the factors $A_{n+1}(\boldsymbol{\sigma},\mathbf{r})$ and $T_{n+1}(\beta\boldsymbol{\sigma},\mathbf{r})$ do not vanish. These are what are known as the G—T terms.

Beta-spectra are usually analyzed in terms of the Kurie plot. For magnetic spectrometers, this is the graph of $[N/p^3F(Z,W)]^{\frac{1}{2}}$ *vs* W, where $P(p)$ is taken to be proportional to N/p, N being the counting rate. For an allowed spectrum the Kurie plot is straight with an intercept equal to W_0. If the Kurie plot is not straight, the spectrum is forbidden, indicating that C_{nX} is not energy independent. The appropriate C_{nX} is then sought which will correct the Kurie plot to a straight line.

II. EXPERIMENTAL DESCRIPTION

The Columbia University spectrometer constructed in 1941 is of the solenoidal type, a complete description of its physical features having been given by Witcher,[9] and subsequent modifications by Haggstrom[10] and Wu and co-workers.[11] Essentially the solenoid consists of six layers of $\frac{1}{4}$-in. diameter copper tubing (0.035-in. wall thickness) wound on a brass tube 10.5-in. o.d., 10-in. i.d., and 66 in. long. The actual length of winding is 60 in. and there are 220 turns per layer. All six layers are connected in parallel, both electrically and hydraulically, by means of bus bars and manifolds. In addition correcting coils consisting of 90 turns of No. 12 wire were wound 12 in. from each end of the main winding to improve the homogeneity of the field inside the solenoid. Comparison measurements with a standard solenoid showed that the homogeneity of the field at all points between the source and counter is better than 1 percent. The defocusing effect of the earth's magnetic field for low energy electrons has been reduced to a negligible amount by aligning the spectrometer tube parallel to the horizontal component of the earth's field and neutralizing the vertical component by means of a pair of Thomson coils (42 in.$\times$100 in.) placed above and below the spectrometer tube.

The long half-lives associated with the highly forbidden spectra implies unavoidable low specific activities and therefore prohibits the use of sources with activities greater than a few hundreths of a microcurie if the distortion of the spectrum shape due to excessive source thickness is to be avoided. To combat the problem of low intensity, a new baffle with improved resolution-transmission characteristics was constructed and several techniques were adopted for reducing the background of the G-M counter detection system. The new baffle was constructed using the design principles for ring-focusing as presented by Frankel[12] and Persico.[13] The existence of the ring-focus for a solenoid was first noted by Witcher, who did not, however, fully exploit its usefulness, since the original baffle was designed to transmit electrons with an average initial angle $\bar{\alpha}$ of 18°. The new baffle, whose physical dimensions are shown in Fig. 1, was designed for $\bar{\alpha}=38°$, $D=2p/eH=14.1$ cm, and $L=\pi D\cos\bar{\alpha}=34.8$ cm. The coordinates of disk A, $r_A=6.7$ cm, $Z_A=24.7$ cm, determine the calibration of the baffle, i.e., the energy of the electrons transmitted for a given magnetic field setting. The resolution and transmission can be varied without changing the baffle calibration by adjusting either or both the r and Z coordinates of disk A'. The factors determining the shape of the slit at AA' and the location of the beam defining diaphragm at either BB' or CC' have been discussed extensively in the literature.[14,15] The baffle was calibrated using the photoelectrons from a lead radiator by the annihilation radiation from the positrons of Cu^{64}, and it was found that $D=14.1$ cm. Subsequent checks with internal conversion lines of Cs^{137}, In^{114}, etc., have shown agreement well within experimental error.

The K and L lines from the internal conversion electrons of In^{114} as obtained with Witcher's baffle and with the new baffle adjusted to give the same resolution are shown in Fig. 2. The half-maximum width is 3.9 percent corresponding to a base width of about 9–10 percent. The increase in transmission achieved by the new baffle is 3.7 as obtained from the ratio of the line peaks. The value of four is predicted for a half-maximum width of 4 percent by Frankel for a point source and by Persico for the case of an extended source. A determination of the average solid angle transmitted by the baffle was obtained by integrating the momentum distribution of a Cl^{36} source whose total activity had been determined by absolute beta-counting. The half-maximum resolution for this source whose diameter is 0.8 cm is 5.8 percent and the average solid angle is 3.5 percent of 4π. The value reported by Witcher is 1 percent maximum solid angle for a source 2.0 cm in diameter with a half-maximum resolution of 5.8 percent.

The large spherical aberration of the solenoidal spectrometer for emission angles of the order of 40° enlarges the beam width to about 5 cm as it returns to the axis. An end-window G-M counter large enough to admit the beam has a prohibitively high background for use with low activity sources. Other type G-M counters or detectors suggest themselves to a solution of this problem, but it was deemed more feasible to attempt to reduce the background of an end-window G-M counter. This was accomplished by two methods. First, the sensitive volume for radiation entering perpendicular to the axis was considerably reduced by using a center wire of 0.006-in. tungsten, 4.0 cm in length, with a glass bead at one end and 0.040-in. Kovar wire butt soldered at the other end to serve as a lead-in (Fig. 3).[16] The sensitive volume of the counter is determined by the length of the 6-mil wire since the counting threshold for the 40-mil wire is above the entire plateau region of the 6-mil wire. The 6-mil wire was further reduced in length to 1.8 cm for spectrum

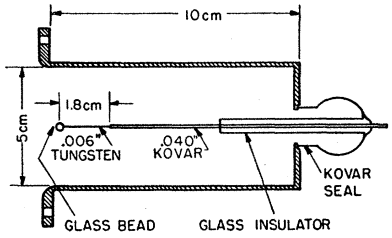

FIG. 3. Cross section of low background, end-window G-M counter.

[9] C. M. Witcher, Phys. Rev. **60**, 32 (1941).
[10] E. Haggstrom, Phys. Rev. **62**, 144 (1942).
[11] Wu, Havens, Albert, and Grimm, Phys. Rev. **73**, 1259 (1948).
[12] S. F. Frankel and E. C. Nelson, ONR Report NP-1120, June, 1948.
[13] E. Persico, Rev. Sci. Instr. **20**, 191 (1949).
[14] S. F. Frankel, Phys. Rev. **73**, 804 (1948).
[15] E. Persico and C. Geoffrion, Rev. Sci. Instr. **21**, 945 (1950).
[16] Good, Kip, and Brown, Rev. Sci. Instr. **17**, 262 (1946).

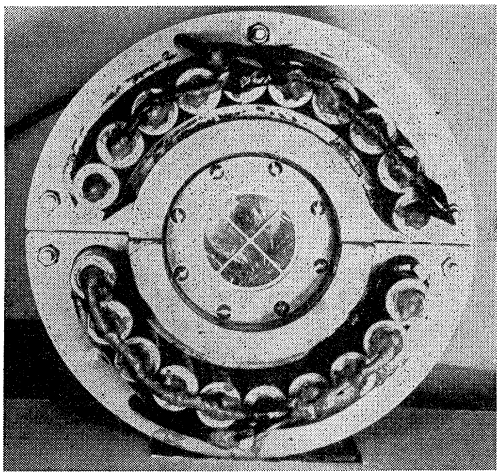

FIG. 4. Cutout showing G-M counter, lead shielding, anticoincidence counters and support.

measurements of K^{40}. Counters constructed in this way, 10 cm long and 5 cm in diameter, have a $1\frac{1}{2}$-in. lead shielded background of 44 c/min for the 4.0-cm wire and 30 c/min for the 1.8-cm wire. The background of these counters was further reduced to 28 c/min and 16 c/min by the use of an anticoincidence counting technique. The counter which serves as the beta-detector is completely surrounded by an array of cosmic-ray counters 1 in. in diameter and 12 in. long (Fig. 4). An anticoincidence circuit was constructed which records counts occurring only in the detector and rejects those detector counts which occur in coincidence with a count in any of the cosmic-ray counters. It was found that the number of counts rejected by this method is roughly independent of the amount of shielding used. This is readily explained by the fact that the components of the background capable of initiating ionizing events in both the cosmic-ray counters and the beta-counter are highly penetrating and unaffected by ordinary amounts of shielding. A gamma-ray, however, will not generally register counts in two counters and is not susceptible to rejection by the anticoincidence technique. The gamma-ray background can be minimized by using the maximum practical amount of shielding.

The thin windows used on the G-M counters are either Nylon or rubber hydrochloride, both of 0.6 mg/cm^2 thickness, and for measurements below 100 kev, five to six layers of collodion films each about 0.006 mg/cm^2 thick. The transmission of the electron beam is not at all affected by the Nylon windows above 90 kev and by collodion windows of about 0.03 mg/cm^2 thickness above 16 kev. The counters are filled with 15 mm of alcohol vapor when the collodion windows are used and with 8–10 cm of a 7:1 argon-alcohol mixture when Nylon windows are used in the investigation of the higher energy regions. Sufficient data are taken so that there is adequate overlap in the regions studied with Nylon and collodion windows. Measurements have shown that the G-M counters when used as described above have close to 100 percent efficiency for detection of beta-particles.[11]

Mechanical support is given to the counter windows by means of grids. If not properly designed, the grids can produce selective transmission effects. The solid parts of the grid should be completely opaque to the most energetic electrons in the beam. The importance of edge effects in the small circular apertures of the grids used to support collodion windows was investigated by comparing the transmission of several grids with varying ratios of aperture diameter to depth. It was found that a ratio of at least 2:1 was necessary to eliminate edge effects for all energies above 20 kev. The grid support for Nylon windows has a circular aperture of 5-cm diameter with two thin perpendicular strips of $\frac{1}{8}$-in. width forming a coordinate axis to support the window. A grid such as this has an open area of about 97 percent and negligible edge affects.

The recent history of beta-ray spectroscopy has stressed the importance of source uniformity as well as low surface density for reproducing accurate spectra. The best method seems to be the vacuum evaporation technique, which consists essentially of placing the source material in a vacuum on a heating strip or small oven. When heated in a high vacuum until its vapor pressure is about 10^{-2} mm of mercury or greater, the source material will volatilize and deposit on thin films placed a short distance away. Unfortunately, most of the substances exhibiting highly forbidden spectra are not available in sufficient quantities for use of the vacuum evaporation technique. The sources used for the Cl^{36} measurements were prepared by this method.[17] All the other sources were prepared in various ways which will be individually described and their limitations discussed.

III. SPECTRUM INVESTIGATIONS

A. Be^{10}

Be^{10} is an even-even nucleus and is assumed to have zero spin, whereas the spin of B^{10}, the product nucleus, has been found to be three.[18] Thus the spin change involved in the transition is three, and the interactions which can account for the decay are C_{2T}, C_{2A}, and C_{3P} if the parity does not change and C_{3S}, C_{3V}, C_{3T}, and C_{3A} if the parity does change. The matrix element $Q_3([\boldsymbol{\alpha}\times\mathbf{r}],\mathbf{r})$ for C_{4V} can also account for a $\Delta J=3$ transition, but this leads to a half-life much higher than the observed value. C_{2T} and C_{2A} are examples of the case $\Delta J=n+1$ and each contains a single matrix element with the same energy factor, $T_3(\beta\boldsymbol{\sigma},\mathbf{r})=A_3(\sigma,\mathbf{r})=(3p^4+10p^2q^2+3q^4)/90$. This factor, which has sometimes been called the D_2 factor, is also contained in matrix elements appearing in C_{3V} and C_{3T}, i.e., $V_3(\boldsymbol{\alpha},\mathbf{r})$

[17] We are indebted to L. Lidofsky and P. Macklin of this laboratory for use of the vacuum evaporator constructed by them.

[18] Gordy, Ring, and Berg, Phys. Rev. 74, 1191 (1948).

and $T_3(\beta\alpha, \mathbf{r})$. There are two bases for predicting that the shape of the Be^{10} spectrum is that given by the D_2 factor. Marshak[19] has shown that only C_{2T}, C_{2A}, C_{3T}, and C_{3V} give minimum theoretical half-lives compatible with the observed value of 2.7×10^6 years. By using Greuling's method for estimating the magnitude of the matrix elements occurring in C_{3T} and C_{3V}, it was shown that in each case the term containing the D_2 factor, i.e., $T_3(\beta\alpha, \mathbf{r})$ and $V_3(\alpha, \mathbf{r})$ is much larger than all the others. Thus C_{3T} and C_{3V} as well as C_{2T} and C_{2A} all lead to the same spectrum shape, that determined by the D_2 factor. This result is obtained more directly from the shell model of the nucleus which predicts no parity change for the transition. Thus $\Delta J=3$ (no) and the possible interactions are restricted to C_{2T} and C_{2A}. Empirically the Be^{10} decay is classified as second forbidden by its f_0T value of 4.6×10^{14} (see Table I).

Experimental evidence that the spectrum shape of Be^{10} deviated from the allowed shape was first reported by Bell *et al.*[20] using a scintillation spectrometer. Wu and Feldman[1] first inferred the D_2 shape of the Be^{10} spectrum by comparing the spectrum shape of thick sources of radioactive BeO ($\sim$10 mg/cm^2) to that of the thick sources of inactive BeO containing activities of Cu^{64} and Cl^{36}. The availability of material of higher specific activity has made possible spectrum measurements with much thinner sources, of about 0.3–0.4 mg/cm^2. The source used in this work was obtained from the Y-12 Research Laboratory of the Carbide and Carbon Chemicals Corporation at Oak Ridge. It was prepared by activating Be metal in the pile and then was purified and isotopically enriched in Be^{10} by electromagnetic separation performed under the supervision of Dr. C. P. Keim. The source was mounted on a Formvar film 0.1 mg/cm^2 thick and consisted of 1.2 mg BeO spread over an area of about 4 cm^2. The activity of this source is about 0.01 microcurie and although fairly thin (0.3 mg/cm^2) is not particularly uniform and could not be expected to give reliable results below 100 kev. The ring-focus baffle has a resolution of 9 percent full width at half-maximum for a source of this diameter. The graph of the momentum distribution has the pronounced shift of the peak towards the high energy end, characteristic of a D_2 spectrum. Figure 5 contains graphs of the Kurie plot and the Kurie plot corrected by the D_2 factor. The uncorrected curve is concave towards the energy axis whereas the D_2 correction factor yields a straight line down to 120 kev and is seen to provide a good fit of the data. The deviation below 120 kev is attributed to source thickness effects. The extrapolated end point is 555±5 kev.

TABLE I. Corrected and uncorrected fT values.

	ΔJ	n	$W_0(mc^2)$	T(sec)	f_0T	f_nT
Tc^{99}	2	2	1.57	0.97×10^{13}[a]	1.7×10^{12}	3.8×10^{11}
Cl^{36}	2	2	2.40	2.01×10^{13}[b]	4.1×10^{13}	1.2×10^{13}
Be^{10}	3	2	2.09	1.23×10^{14}[c]	4.6×10^{14}[e]	1.3×10^{12}[e]
K^{40}	4	3	3.60	5.79×10^{16}[d]	1.3×10^{18}	1.4×10^{15}

[a] Fried, Jaffey, Hall, and Glendenin, Phys. Rev. **81**, 741 (1951).
[b] D. J. Hughes and C. Eggler, Phys. Rev. **74**, 1239 (1948).
[c] Wu, Townes, and Feldman, Phys. Rev. **76**, 692 (1949).
[d] G. A. Sawyer and M. L. Wiedenbeck, Phys. Rev. **79**, 490 (1950).
[e] These values contain the factor $(2J_f+1)/(2J_i+1)=7$ because $J_f>J_i$.

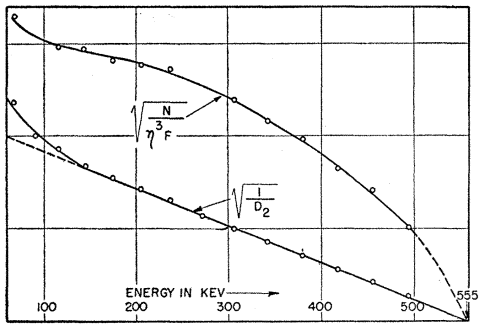

FIG. 5. Corrected and uncorrected Kurie plots Be^{10} spectrum.

These results are in essential agreement with those reported by other laboratories, the main difference being the point at which the low energy deviation sets in. This can be explained for the most part by the difference in uniformity and thickness of the sources used. Hughes, Eggler, and Alburger[21] using a thin lens spectrometer with a resolution of $\sim$18 percent found the D_2 corrected Kurie plot to be straight down to 180 kev. The results reported by Bell and Cassidy[22] obtained with a scintillation spectrometer show that the deviation sets in at 250 kev. This deviation at energies higher than would be expected from source thickness effects has been attributed to a scattering effect from the crystal.[23] Fulbright and Milton[24] using a proportional counter and sources varying from 0.5 to 3.5 mg/cm^2 of BeO, obtained agreement with the D_2 shape down to 100 kev.

The curves for the various correction factors applicable to the Be^{10} decay have been given by Marshak.[19] The experimental shape of the Be^{10} spectrum above 120 kev is in such close agreement with the D_2 shape that by inspection it is possible to exclude C_{3P}, C_{3S}, and C_{3A} as possible interactions. It can be further concluded that if the parity does change, requiring the transition to be third forbidden, then the terms in C_{3T} and C_{3V} other than the D_2 term ($T(\beta[\boldsymbol{\sigma}\times\mathbf{r}], \mathbf{r})$, $V(\mathbf{r}, \mathbf{r})$ and the cross terms) must be negligibly small compared to the D_2 term. Thus it is seen that the Be^{10} spectrum provides a decisive confirmation of the Fermi theory exhibiting the unique shape predicted by Marshak's lifetime analysis for a spin change of three.

[19] R. E. Marshak, Phys. Rev. **75**, 513 (1949).
[20] Bell, Ketelle, and Cassidy, Phys. Rev. **76**, 574 (1949).
[21] Hughes, Eggler, and Alburger, Phys. Rev. **77**, 726 (1950).
[22] P. R. Bell and J. M. Cassidy, Phys. Rev. **77**, 301 (1950).
[23] B. H. Kettelle, Phys. Rev. **80**, 758 (1950).
[24] H. W. Fulbright and J. C. D. Milton, Phys. Rev. **76**, 1271 (1949).

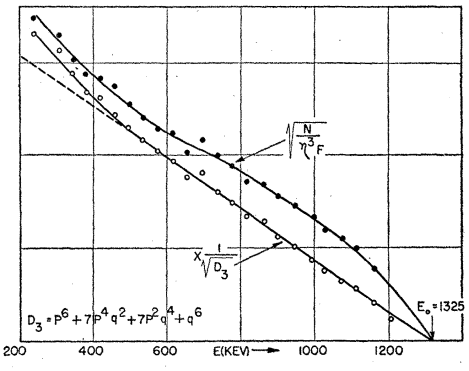

FIG. 6. Corrected and uncorrected Kurie plots of K^{40} spectrum for 2.5-mg/cm² source.

B. K^{40}

The measurement of the K^{40} beta-spectrum, a case of a highly forbidden transition for which the spin change is known, has long been anticipated as a sensitive test for the Fermi theory. The spin change is $\Delta J=4$, that of K^{40} having been found to be four,[25] while that of Ca^{40}, the product nucleus, is assumed to be zero because it is an even-even nucleus.

K^{40} occurs naturally with an abundance of 0.016 percent and since its half-life is 12.7×10^8 years, it has not been possible to prepare sources of sufficiently high specific activity necessary for a spectrum determination. Recently we obtained some KCl enriched to 7.13 percent in K^{40} by electromagnetic separation performed at Oak Ridge under the supervision of C. P. Keim. The source was prepared by precipitating the KCl out of a saturated water solution with a large volume of isopropyl alcohol to which a small amount of alcohol soluble Nylon was added as a binding agent. The uniform crystals formed in this way were allowed to settle from the alcohol over a circular area of 3.1 cm² on Nylon backing of 0.6 mg/cm² thickness. The average source thickness is about 2.5 mg/cm². This technique for preparing thick sources was found to produce greater uniformity than several other methods that were tried. The ring-focus baffle for a source of this diameter has a resolution of 9 percent.

The uncorrected Kurie plot, shown in Fig. 6, is definitely forbidden, its shape being very similar to those of Cl^{36} and Be^{10}. The factor $D_3=p^6+7p^4q^2+7p^2q^4+q^6$, provides a good fit to the data from the end point, 1325 ± 15 kev down to 500 kev with the deviation increasing towards lower energies. This deviation is readily explained by the excessive thickness of the source. To determine the effect of 2.5 mg/cm² KCl on beta-spectra with end points in the neighborhood of 1.3 Mev, a source was prepared identical to the K^{40} source using inert KCl containing Y^{91} activity of negligible weight. The Kurie plot for this source corrected by the factor $a\sim p^2+q^2$ is shown in Fig. 7 together with the uncorrected Kurie plot. For a thin source the a factor corrected Kurie plot would be straight to below 50 kev. The effect of the 2.5 mg/cm² KCl on the Y^{91} spectrum is to produce a deviation which sets in at 500 kev similar to that observed for the K^{40} Kurie plot corrected by the D_3 factor. It can therefore be assumed that the data above 500 kev is unaffected by the source thickness of 2.5 mg/cm² and that with thin sources, the D_3 factor will provide a good fit to the Kurie plot to energies below 500 kev. These results are in general agreement with thick source ($\sim$2.5 mg/cm²) spectrum measurements of K^{40} reported by other laboratories. Alburger[26] using a thin lens with a resolution of about 17 percent found agreement with the D_3 corrected Kurie plot down to about 500 kev. Bell, Weaver, and Cassidy[27] using a scintillation spectrometer found the deviation to begin at about 700 kev.

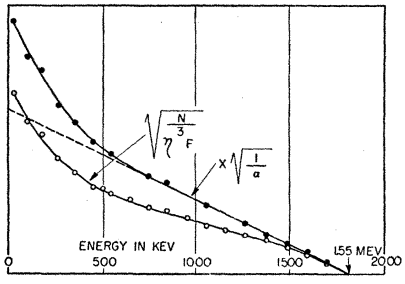

FIG. 7. Corrected and uncorrected Kurie plots of Y^{91} spectrum. Source consists of Y^{91} activity mixed with 2.5-mg/cm² KCl.

For $\Delta J=4$ the possible correction factors are C_{3T}, C_{3A}, and C_{4P} if the parity changes and C_{4S}, C_{4V}, C_{4T}, and C_{4A} for no parity change. The energy factors for these have been previously given by Marshak.[28] Of these C_{3T}, C_{3A}, C_{4P}, C_{4S}, and C_{4A} contain but one matrix element, and therefore the energy dependence for each is uniquely defined. C_{4P}, C_{4S}, and C_{4A} can be ruled out because their energy dependent factors are markedly different from the D_3 factor. The D_3 factor also occurs in C_{4T} and C_{4V} ($T_4(\beta\boldsymbol{\alpha},\mathbf{r})$ and $V_4(\boldsymbol{\alpha},\mathbf{r})$) and is the same unique energy factor in C_{3T} and C_{3A} ($T_4(\beta\boldsymbol{\sigma},\mathbf{r})$ and $A_4(\boldsymbol{\sigma},\mathbf{r})$). In a manner completely analogous to that used by Marshak in analyzing the case of Be^{10} it can be shown that the terms in C_{4V} and C_{4T} containing the D_3 factor are much larger than the other terms and therefore the energy dependence of C_{4T} is essentially that determined by the D_3 factor. By using Greuling's[7] method for estimating the magnitude of the matrix elements one obtains $|Q_4(\beta[\boldsymbol{\sigma}\times\mathbf{r}],\mathbf{r})/4!|^2\approx(2/7)R^8$ and $|Q_4(\beta\boldsymbol{\alpha},\mathbf{r})/4!|^2\approx(18/35)\alpha^2R^6$. If we use $R=0.004A^{\frac{1}{3}}$ for the nuclear radius and $\alpha^2=(v/c)^2=0.1-(W_0R)^2$, the ratio of the second term to the first in C_{4V} is $9\alpha^2T_4(\beta\boldsymbol{\alpha},\mathbf{r})/5R^2T_4(\beta\boldsymbol{\sigma}\times\mathbf{r},\mathbf{r})$, which is $\approx10^3T_4(\beta\boldsymbol{\alpha},\mathbf{r})/T_4(\beta\boldsymbol{\sigma}\times\mathbf{r},\mathbf{r})$. The variation in $T_4(\beta\boldsymbol{\alpha},\mathbf{r})/T_4(\beta\boldsymbol{\sigma}\times\mathbf{r},\mathbf{r})$ is negligible over the entire spectrum compared to 10^3. Thus the first term in C_{4T} and

[25] J. R. Zacharias, Phys. Rev. **60**, 168 (1941).

[26] D. E. Alburger, Phys. Rev. **78**, 629 (1950).

[27] Bell, Weaver, and Cassidy, Phys. Rev. **77**, 399 (1950).

[28] R. E. Marshak, Phys. Rev. **70**, 980 (1946).

also the cross term (since it can be taken as the geometric mean) are seen to be negligible compared to the term containing the $T_4(\beta\alpha, \mathbf{r})=D_3$ factor. The matrix element for the term in $T_{4'}(\beta\sigma, \mathbf{r})$ doesn't apply for a $n\rightarrow 0$ transition. Therefore C_{4T} is essentially determined by one matrix element with its energy dependence given by the D_3 factor. The result for C_{4V} is exactly the same. Thus the spectrum of K^{40} can be explained equally well by C_{3A}, C_{3T}, C_{4V}, and C_{4T}. It is to be noted that these are the interactions which can account for the half-life of K^{40} as calculated by Greuling.[7] According to the shell model the parity should change in the beta-decay of K^{40}, in which case only C_{3T} and C_{3A} can account for the transition.

The reliability of the observed spectrum, because of excessive source thickness, is good only down to 500 kev. Therefore, these conclusions must be deferred until spectrum measurements can be made with thinner sources and the spectral shape below 500 kev can be determined.

C. Tc^{99}

Tc^{99}, a product of uranium fission, has a half-life of 2.12×10^5 years. Its comparative half-life is $f_0T=1.7\times10^{12}$ and the decay is thus empirically classified as second forbidden. The spin and magnetic moment of the ground state of Tc^{99} have been measured[29] confirming it to be a $g_{9/2}$ state as predicted by the nuclear shell model. Further, the shell model classifies the product Ru^{99} as either $d_{5/2}$ or $g_{7/2}$. In either case there is no change in parity, and since a $g_{9/2}\rightarrow g_{7/2}$ transition would be allowed and incompatible with the observed lifetime, the transition is believed to be $g_{9/2}\rightarrow d_{5/2}$. Thus it is second forbidden, with $\Delta J=2$ (no) in agreement with the empirical classification of forbiddenness.

Tc^{99} of specific activity 1.7 μc/mg was obtained from the Isotope Division of the Atomic Energy Commission in the form of NH_4TcO_4. Several sources with average thickness varying from about 0.05 to 0.15 mg/cm² were prepared on collodion films of about 0.02 mg/cm² thickness by drying the aqueous solution under a heat lamp or in a vacuum desiccator. The source thickness was estimated from a measurement of the source activity and the specific activity of the material as given on the isotope packing slip. The NH_4TcO_4 is chemically purified at Oak Ridge but to ensure purity some of the sources were prepared from material which had gone through additional chemical purification and electroplating.

The resolution for the spectrum measurements of Tc^{99} was about 5 percent varying about ±1 percent with the diameter of the several sources used. The uncorrected Kurie plot exhibits a forbidden shape curving concave towards the energy axis. The curves of the energy factors which apply for a $\Delta J=2$ (no) transition are shown in Fig. 8. None of these factors provides

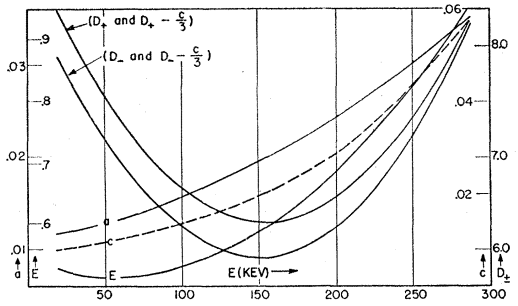

FIG. 8. Correction factors for the individual matrix elements of second forbidden transitions for Tc^{99} ($I=9/2\rightarrow I=5/2$).

a satisfactory fit for the Kurie plot. The D_2 factor overcorrects the Kurie plot, resulting in a curvature in the opposite direction. The a factor gives agreement but only down to about 120 kev, with a deviation that increases towards lower energies setting in at this point. The high Z formulas were used to calculate the correction factors and Coulomb function. The low Z approximation formulas begin to introduce significant errors for $A\sim100$. For Tc^{99}, the error for some of the factors was as much as 10–15 percent over the range where data were taken. A good fit for the Kurie plot is obtained with C_{2T} which for a $J=9/2\rightarrow J=5/2$ transition is[30]

$$C_{2T}=T_2(\beta[\boldsymbol{\sigma}\times\mathbf{r}], \mathbf{r})+k^2T_2(\beta\alpha, \mathbf{r}) -2kT_2(\beta\alpha, \mathbf{r}:\beta[\boldsymbol{\sigma}\times\mathbf{r}], \mathbf{r})+m^2T_2(\beta\sigma, \mathbf{r}) \quad (3a)$$

or in the notation of Konopinski's review article[8]

$$C_{2T}=(D_+-\tfrac{1}{3}c)+12ak^2-4Ek+cm^2, \quad (3b)$$

where

$$k^2=|Q_2(\beta\alpha, \mathbf{r})|^2\div|Q_2(\beta[\boldsymbol{\sigma}\times\mathbf{r}], \mathbf{r})|^2=|A_{ij}|^2\div|T_{ij}|^2$$

and

$$9m^2=|Q_3(\beta\sigma, \mathbf{r})|^2\div|Q_2(\beta[\boldsymbol{\sigma}\times\mathbf{r}], \mathbf{r})|^2=|S_{ijk}|^2\div|T_{ij}|^2.$$

The corrected Kurie plots for the various sources used, shown in Fig. 9, are straight down to about 60 kev. Measurements below 50 kev were unreliable because of

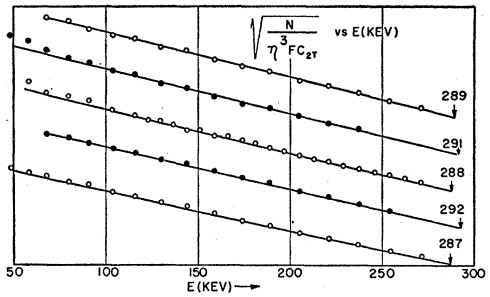

FIG. 9. Tc^{99} Kurie plots corrected by C_{2T} with $k^2=|A_{ij}|^2/|T_{ij}|^2=45$.

[29] K. G. Kessler and W. F. Meggers, Phys. Rev. **80**, 901 (1950); **82**, 341 (1951).

[30] The requirement that $k=A_{ij}/T_{ij}=A_{ij}^*/T_{ij}^*$ is a consequence of the invariance of the nuclear Hamiltonian under time reversal. The proof is given by C. L. Longmire and A. M. L. Messiah, Phys. Rev. **83**, 464 (1951).

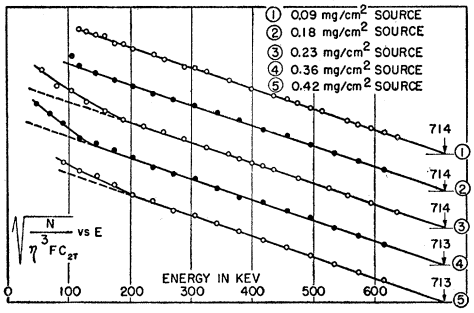

FIG. 10. Cl^{36} Kurie plots corrected by C_{2T} with $k^2=|A_{ij}|^2/|T_{ij}|^2=18$.

the low source activities. The extrapolated end point is 290±4 kev. The best fit was obtained with $k^2=45$ and $m^2=0$. The term in m^2, although permissible by the selection rules, is negligibly small since $c/(D_+-\frac{1}{3}c)$ $\approx 0.002-0.003$ over most of the spectrum and is at most 0.006 at the high energy end, while $m^2\approx 14/15$ according to Greuling's method for approximating the matrix elements.

Past experience in beta-spectroscopy has shown that very thin sources prepared by drying from aqueous solution do not always give reliable measurements at low energies because of inhomogeneities in surface density. Confirmation is required by measurements obtained with sources that are known to be very uniform as well as thin. A spectrum measurement of Tc^{99} was reported at the last American Physical Society meeting in New York[31] using a source prepared by the oven volatilization technique. It was found that a good fit to the spectrum down to 50 kev was provided by C_{2T} with $k^2=44$ in agreement with the results reported herein. The spectrum of Tc^{99} has also been investigated by Taimuty[32] and was fitted with C_{2T} by Nakamura *et al.*[33] The exact point of deviation caused by source scattering depends on the end point of the spectrum, on the atomic number of the nucleus responsible for the scattering, and on the thickness and uniformity of the source. Scattering effects for thin sources do not affect the spectrum shape for energies above the peak of the momentum distribution. The point of deviation always occurs at an energy somewhere to the left of the peak. Sixty kev occur to the left of the peak of the Tc^{99} momentum distribution at a momentum of about 0.4 that of the end point. On this basis it seems reasonable that no source scattering effects should be observed down to 60 kev with sources whose average thickness is as low as those used in this work.

D. Cl^{36}

We have previously published results on the spectrum of Cl^{36} [4] using sources of 0.3 to 1 mg/cm² average thickness prepared from aqueous solution by evaporation under a heat lamp or in a vacuum desiccator. The spin of Cl^{36} has been found to be two[34,35] while the product nucleus A^{36}, being even-even, is assumed to have zero spin. The possible interactions for a $\Delta J=2$ transition are C_{1A}, C_{1T}, C_{2P}, C_{3V} if the parity changes and C_{2S}, C_{2V}, C_{2T}, and C_{2A} if there is no parity change. As has been discussed previously,[4] all of these except C_{2T} and C_{2V} consist of but one matrix element and hence have a unique energy dependence (see reference 4 for the curves of the correction factors for Cl^{36}). However, only C_{2T} and C_{2V} with a suitable adjustment of the matrix elements can account for the Cl^{36} beta-spectrum.

We have reinvestigated the spectrum of Cl^{36} using sources of $NaCl^{36}$ of 0.08, 0.15, 0.19, 0.28, and 0.36 mg/cm² average thickness prepared by the vacuum evaporation technique. These sources are much thinner and considerably more uniform than those used in the earlier work. The source thickness was determined from the specific activity of the Cl^{36} given on the isotope invoice sheet together with a determination of the total activity of each source. The resolution of the ring-focus baffle for these sources which are 8 mm in diameter is 5.5 percent. The results are in complete agreement with our previously published results. We again find that C_{2T} (as well as C_{2V}) as given by Eq. (3) with $k^2=18$ and $m^2=0$ provides a good fit to the spectrum and with the improvement in the sources the corrected Kurie plot is now straight down to 100 kev. The extrapolated end point is 714±5 kev. The term in m^2 is prohibited by the selection rules in this case because the transition is of the $n\rightarrow 0$ type. The low activity of the sources made measurements below 100 kev impractical. The Kurie plots corrected by C_{2T} are shown in Fig. 10.

The Cl^{36} spectrum has been determined down to about 180 kev by Fulbright and Milton[36] using a proportional counter. They were able to fit the spectrum with C_{2T} for $k^2=25.73$. Our data cannot be fitted with a ratio this high in the region below 300 kev, corresponding to a relatively greater number of electrons at low energies than in the spectrum measurements of Fulbright and Milton.

IV. DISCUSSION

The half-life and fT values for the spectra investigated are given in Table I. Both f_0 and f_n were obtained by graphical integration of

$$f_n=\int_1^{W_0} C_{nX}F(Z,W)(W^2-1)^{\frac{1}{2}}(W_0-W)^2WdW.$$

Every term in this formula has been previously tabulated as a function of W in the interpretation of the

[31] F. Wagner, Jr., and M. S. Freedman, Phys. Rev. **86**, 631 (1952).
[32] S. I. Taimuty, Phys. Rev. **81**, 461 (1951).
[33] Nakamura, Umezawa, and Takebe, Phys. Rev. **83**, 1273 (1951).
[34] C. H. Townes and L. C. Aamodt, Phys. Rev. **76**, 695 (1949).
[35] Johnson, Gordy, and Livingston, Phys. Rev. **83**, 1249 (1951).
[36] H. W. Fulbright and J. C. D. Milton, Phys. Rev. **82**, 274 (1951).

spectrum shape, and therefore it is both simple and accurate to obtain f_0 and f_n by graphical integration. The values thus obtained for f_0 are in close agreement with those given in the f_0 charts of Feenberg and Trigg.[37] The f_0T correspond to $C_{0X}=1$, whereas the f_nT are calculated using the C_{nX} which is in best agreement with the spectrum. The factors $(n!)^2$ and $[(n+1)!]^2$ which appear in the denominators of the C_{nX} are 4, 4, 36, and 576, respectively, for Tc^{99}, Cl^{36}, Be^{10}, and K^{40}. It is these factors which are responsible for the greater reduction in the ratio of f_nT/f_0T for Be^{10} and K^{40} compared to Tc^{99} and Cl^{36}. The low end point of the Tc^{99} spectrum causes a relatively greater reduction in its f_nT value than in the case of Cl^{36}.

According to Greuling's method for approximating the matrix elements the value of k^2 should be $5(\gamma_5)^2/9R^2$. With γ_5^2 having a value probably between 0.01 and 0.1, k^2 is then between 30 and 300 for Cl^{36} and 18 to 180 for Tc^{99}. The values used for the best spectrum fit are 18 and 45, respectively. It might be noted that Greuling's method successfully accounts for the lifetimes of Be^{10} and K^{40} but yields values for Cl^{36} and Tc^{99} (assuming the interaction is $2T$) that are too low by a factor of the order of 100.

It is of interest to note that although the spin changes for the decays of Cl^{36}, Be^{10}, and K^{40} are 2, 3, and 4, respectively, and the spectrum shapes are explained by C_{2T} with $k^2=18$ for Cl^{36}, by the D_2 factor for Be^{10}, and by the D_3 factor for K^{40}, these three spectra have essentially the same energy dependence to within the accuracy of the measurements.

As a result of these spectrum investigations it is possible to arrive at the following analysis concerning the interaction prevailing in beta-decay. If the true interaction is just a single one of the five linearly independent interactions of Eqs. (2), then the tensor interaction is the only one which can satisfactorily account for spectra in which the change in angular momentum is equal to the degree of forbiddenness, i.e., $\Delta J=n$, as well as those spectra for which $\Delta J=n+1$. The polar vector interaction is exactly the same as the tensor for the case $\Delta J=n$ if one takes $A_{ij}/R_{ij}=2iA_{ij}/T_{ij}$, but is forbidden by the selection rules for the case $\Delta J=n+1$. The axial vector interaction is identical to the tensor interaction for the case $\Delta J=n+1$ but cannot explain the shape of forbidden spectra with $\Delta J=n$ (e.g., Cl^{36}, Tc^{99}). Although the tensor interaction seems to be able to explain the experimentally observed shapes of these forbidden spectra, there is so much flexibility available in the use of the parameter k^2 to fit the experimental data that no final conclusions should be drawn. Furthermore, a linear combination of the tensor interaction with an admixture of Fermi terms will serve as well as the tensor alone in the interpretation of the shapes of forbidden spectra. A linear combination of T and P has been used by Petschek and Marshak[38] to fit the shape of the RaE spectrum assuming the transition is $0\rightarrow0$ with change in parity. As was pointed out, the P interaction would give negligibly small contributions to the combination in all except $0\rightarrow0$ transitions because its terms would always be smaller in magnitude than those of the T interaction by two degrees of forbiddenness. The S and V interactions are prohibited by the selection rules for a $0\rightarrow0$ (yes) transition, and hence this type of transition cannot detect the presence of Fermi terms in the interaction prevailing in beta-decay. It has been shown by Tolhoek and de Groot[39] that the only linear combinations which can satisfy the condition of invariance of the beta-process to time reversal and possess complete symmetry of positron and negatron emission are either V and T only, or S, A, and P only. On the other hand, various authors have proposed a universal Fermi interaction between spin $\frac{1}{2}$ particles so that the interaction constant would be the same for the beta-decay of the neutron ($n\rightarrow p+e+\nu$), the spontaneous decay of the μ meson ($\mu^-\rightarrow e+2\nu$), and μ-meson absorption ($p+\mu^-\rightarrow n+\nu$). The only combinations consistent with this assumption are either V and A or S, T, and P. These combinations are incompatible with the symmetry principle of Tolhoek and de Groot.

If a linear combination of the invariant interactions does prevail in beta-decay then additional information will be required to determine its exact form. The sources which seem best able to provide the necessary data are the investigation of the shapes of parity unfavored spectra, i.e., $\Delta J=n$ or $\Delta J=n-1$ (especially $0\rightarrow0$ transitions) and various nuclear angular correlation measurements, particularly the electron-neutrino angular correlation. Further, any such linear combination should yield a consistent scheme of fT values.

[37] E. Feenberg and G. Trigg, Revs. Modern Phys. **22**, 399 (1950).

[38] A. G. Petschek and R. E. Marshak, Phys. Rev. **85**, 698 (1952).

[39] H. A. Tolhoek and S. R. de Groot, Phys. Rev. **84**, 150 (1951); L. C. Biedenharn and N. E. Rose, Phys. Rev. **83**, 459 (1951); S. R. de Groot and H. A. Tolhoek, Physica **16**, 456 (1950).

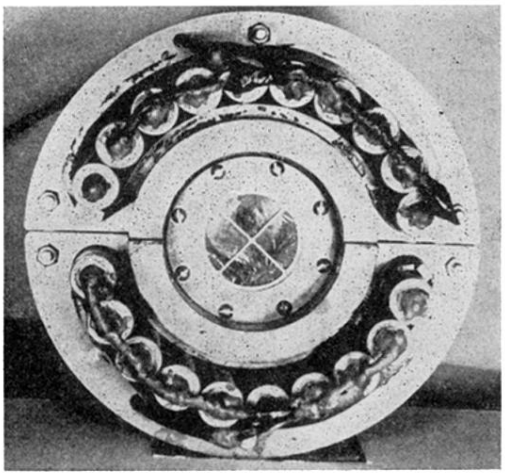

FIG. 4. Cutout showing G-M counter, lead shielding, anticoincidence counters and support.